Available online at www.sciencedirect.com
ScienceDirect
Solar Energy xxx (2008) xxx–xxx
SOLAR ENERGY
www.elsevier.com/locate/solener

Experimental investigation of optimum thermohydraulic performance of solar air heaters with metal rib grits roughness

S.V. Karmare [a,*], A.N. Tikekar [b]

[a] Department of Mechanical Engineering, Government College of Engineering, Shivaji University, Kolhapur, Karad, Maharashtra 415 124, India
[b] Department of Mechanical Engineering, Walchand College of Engineering, Shivaji University, Kolhapur, Sangli, 416416 Maharashtra, India

Received 7 October 2006; received in revised form 19 December 2007; accepted 8 May 2008

Communicated by: Associated Editor G.N. Tiwari

Abstract

Artificial roughness has been found to enhance the heat transfer from the collector plate to the air in a solar air heater. However, it would result in increase in frictional losses and hence, power required by fan or blower. This paper presents the results of an experimental investigation of thermohydraulic performance of roughened solar air heaters with metal rib grits. The range of variation of system and operating parameters is investigated within the limits of, e/D_h: 0.035–0.044, p/e: 15–17.5 and l/s as 1.72, against variation of Reynolds number, Re: 3600–17000. The study shows substantial enhancement in thermal efficiency (10–35%), over solar air heater with smooth collector plate. The thermal efficiency enhancement is also accompanied by a considerable increase in the pumping power requirement due to the increase in the friction factor (80–250%). The optimum design and operating conditions have been determined on the basis of thermohydraulic considerations. It has been found that, the systems operating in a specified range of Reynolds number show better thermohydraulic performance depending upon the insolation. A relationship between the system and operating parameters that combine to yield optimum performance has been developed.

Keywords: Heat transfer; Roughness; Metal rib grit; Turbulent; Solar air heater

1. Introduction

The use of artificial roughness on a surface is an effective technique to enhance the rate of heat transfer to fluid flowing in a duct (Hosni et al., 1991; Dipprey and Sabersky, 1963; Han, 1984; Webb and Eckert, 1972; Han and Zhang, 1992; Liou and Hwang, 1993). Turbulence promoters or roughness elements have been used to improve the convective heat transfer by creating turbulence in the flow. However, it would result in an increase in friction losses and hence, greater power requirement by fan or blower. In order to keep the friction losses at a minimum level, the turbulence must be created only in the region very close to the duct surface i.e. in laminar sub-layer. The surface roughness can be produced by several methods, such as sand blasting, machining, casting, forming, welding ribs and by fixing thin circular wires along the surface(metal rib grits).

It has been recently proposed by several investigators that provision of artificial roughness on the underside of absorber plate could substantially enhance the heat transfer capability of a solar air heater. Prasad and Mullick (1983) utilized artificial roughness in a solar air heater in the form of small wire to increase the heat transfer coefficients. Prasad and Saini (1988) investigated fully developed turbulent flow in a solar air heater duct with a small diameter profusion wire on the absorber plate. Gupta Dhananjay et al. (1997) used continuous ribs of inclination 60° and they

* Corresponding author. Tel.: +91 02164 272901; fax: +91 02164 271713.
E-mail address: karmaresv@rediffmail.com (S.V. Karmare).

0038-092X/$ - see front matter © 2008 Published by Elsevier Ltd.
doi:10.1016/j.solener.2008.05.017

Nomenclature

A_c	smooth plate heat transfer area, WL_f, [m^2]
A_o	orifice area, πr^2, [m^2]
C_d	coefficient of discharge
C_p	specific heat of air, [J/kg K]
c	$\eta_F \eta_m \eta_{tr} \eta_{th}$
D_h	hydraulic diameter of duct, 4WH/2(W + H), [m]
e	metal grit roughness height, [mm]
e/D_h	relative roughness height,
f, f	fanning friction factor,
F	plate efficiency factor,
h	convective heat transfer coefficient between the collector& air, [W/m^2 K]
H	air flow duct depth, [mm]
I	intensity of solar radiation, [W/m^2]
K	thermal conductivity of air, [W/m K]
L_f	length of test section, [m]
l	projected length of metal rib grit perpendicular to direction of flow, [m]
s	projected length of metal rib grit parallel to direction of flow, [m]
l/s	relative length of metal rib grit
m	mass flow rate, [kg/s]
Nu	Nusselt number,
p	metal grit rib pitch, [mm]
p/e	relative roughness pitch,
Pr	Prandtl number,
ΔP_o	pressure drop in orifice, [Pa]
ΔP_d	pressure drop in duct, [Pa]
P_m	mechanical energy consumed for propelling air through collector, [W]
Q	heat transfer rate, [W]
Re	Reynolds number,
St	Stanton number,
T_a	ambient temperature, [°C]
T_i	air inlet temperature, [°C]
T_{fm}	bulk mean temperature, [°C]
T_o	air outlet temperature, [°C]
T_{pm}	mean plate temperature, [°C]
$T_1 - T_{10}$	plat temperatures, [°C]
U_L	overall heat loss coefficient, [W/m^2 k]
V	velocity of air in duct, [m/s]
V_w	wind velocity, [m/s]
W	width of duct, [m]
W/H	aspect ratio of duct.

Greek symbol

ρ	density of air, [kg/m^3]
θ	rib angle of attach, [degree]
η_{eff}	Effective efficiency
$\tau\alpha$	transmittance absorptance product for absorber cover combination

Suffix

s	smooth surface

optimized thermohydraulic performance. They found that the optimum operating flow rate shifted to a lower value as the relative roughness height increases. Karwa et al. (1999) used chamfered rib roughness on the absorber plate and they found that at low flow rate, the solar air heater with roughness elements having a higher relative roughness height yields a better performance. However, it has been observed that the fixing of small wires along the absorber plate is a tedious task and may not be economically feasible (Saini and Saini, 1997). A suitable geometry of roughness element therefore needs to be selected, which besides being easily available should be easy to fix on the absorber plate. A commercially available wire mesh or expanded metal matrix has been thought to be one such appropriate alternative.

As implied from the discussion of the effect of rib roughness, the heat transfer coefficient enhancement is also accompanied with an enhancement in the friction factor. Thus, an appropriate way to evaluate performance, in the case of solar air heaters with a roughened absorber plate, is to take both heat collection rate and pumping power requirement into account, i.e. to carry out a thermohydraulic performance evaluation.

The objective of the present investigation is to study, both theoretically and experimentally, the effect of metal rib grits on absorber plate at 60° of angle of attack to the flow direction of air, on the thermohydraulic performance of solar air heater.

2. Thermohydraulic performance

Effective efficiency η_{eff} of the collector is computed from the relation

$$\eta_{eff} = (q_u - P_m/c)IA_c \quad (1)$$

where $c = \eta_F \eta_m \eta_{tr} \eta_{th}$ and the rate of useful thermal energy is calculated from the equation:

$$q_u = F[I(\tau\alpha) - U_L(T_o - T_i)/2]A_c \quad (2)$$

where $F = [h/(h + U_L)]$ The rate of useful energy gain in a roughened solar air heater may also be calculated from the following equations:

$$q_u = hA_c(T_{pm} - T_{fm}) \quad (3)$$

or

$$q_u = mC_p(T_o - T_i) \quad (4)$$

The mechanical power consumed is given by the expression:

$$P_m = VA\Delta P_d \quad (5)$$

Please cite this article in press as: Karmare, S.V., Tikekar, A.N., Experimental investigation of optimum thermohydraulic performance..., Sol. Energy (2008), doi:10.1016/j.solener.2008.05.017

where $\Delta P_d = (2fLV^2\rho)/D_h$ The correlations for friction factor f and Nusselt number Nu for the metal rib grits roughness were developed by data collection of same roughness surfaces by indoor test in the laboratory (Karmare and Tikakar, 2007). These correlations are given in the Eqs. (6) and (7), respectively.

$$f = 15.55 \times (Re)^{-0.26} \times (e/D_h)^{0.91} \times (l/s)^{-0.27} \times (p/e)^{-0.51}, \text{ for, } 3600 < Re < 17000 \quad (6)$$

$$Nu = 2.4 \times 0^{-3} \times (Re)^{1.3} \times (e/D_h)^{0.42} \times (l/s)^{-0.146} \times (p/e)^{-0.27}, \text{ for, } 3600 < Re < 17000 \quad (7)$$

By substituting for power consumption P_m, from Eq. (5), and q_u, from Eq. (3), into Eq. (1), the following equation is obtained for computation of effective efficiency for a solar air heater:

$$\eta_{eff} = \{F[I(\tau\alpha) - U_L(T_o - T_i)/2]A_c - \rho f L V^3 (W + H)/c\}/IA_c \quad (8)$$

Eq. (8) can also be used for determination of the effective efficiency for a solar air heater with a smooth collector surface. The friction factor and heat transfer coefficient for a smooth collector surface may be obtained from the Blasius (9) and the Dittus- Boelter (10) equations respectively.

$$f_s = 0.079(Re)^{-0.25} \quad (9)$$

$$h_s = 0.023(k/D_h)(Re)^{0.8}(Pr)^{0.6} \quad (10)$$

The effective efficiency η_{eff} of solar air heater with smooth collector surface is computed from the following equation.

$$\eta_{eff} = \{F_s[I(\tau\alpha) - U_{LS}(T_o - T_i)2]A_c - \rho f_s L V^3 (W + H)/c\}IA_c$$
$$F_s = h_s(h_s + U_{LS}) \quad (11)$$

The values of effective efficiency have been computed for a set of system and operating parameters (relative roughness height, Reynolds number and insolation) for duct geometry of 250 mm width, 25 mm depth and 1.5 m length.

3. Experimental procedure

The schematic layout of experimental setup is shown in Fig. 1. The setup is designed according to the ASHARE standard 93-77 for testing of solar collectors (ASHRAE, 1977). The experimental setup consists of two identical collectors with necessary duct of aspect ratio 10 (250 mm × 25 mm) and a centrifugal blower to provide the air from its suction side. The positions of the temperature sensors are shown in Fig. 2. To maintain hydraulic diameter ratio of more than 30, the test section length for collector is

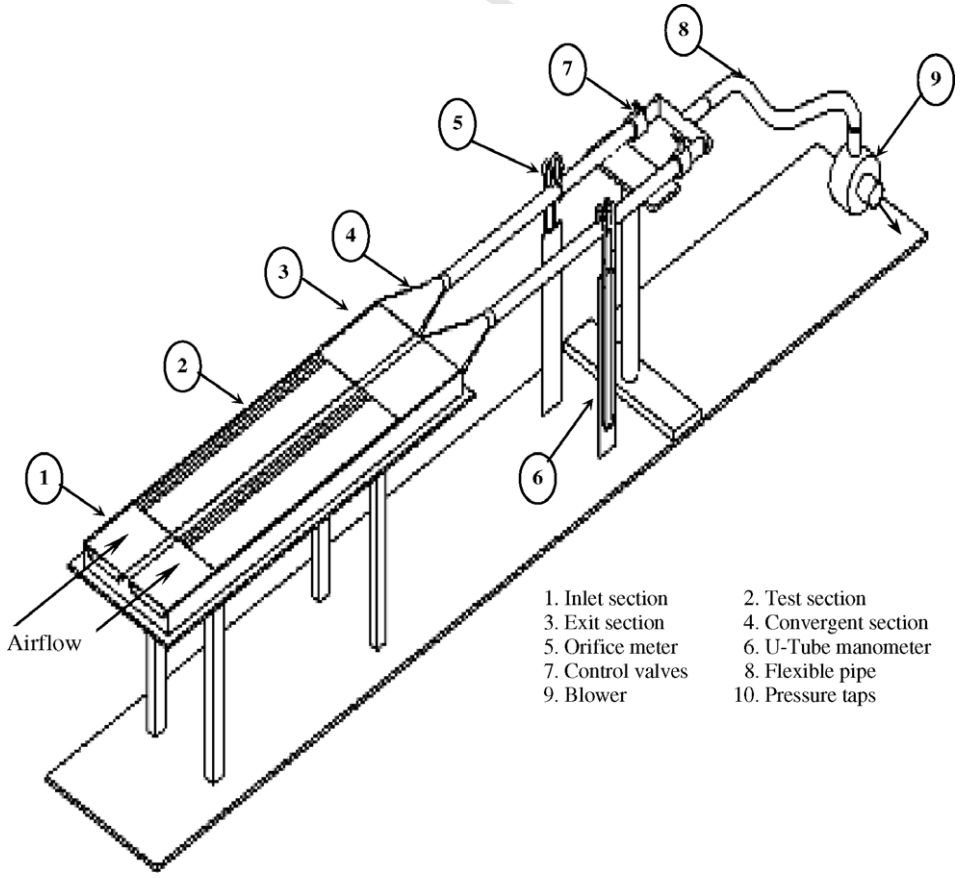

Fig. 1. Schematic layout of the experimental setup.

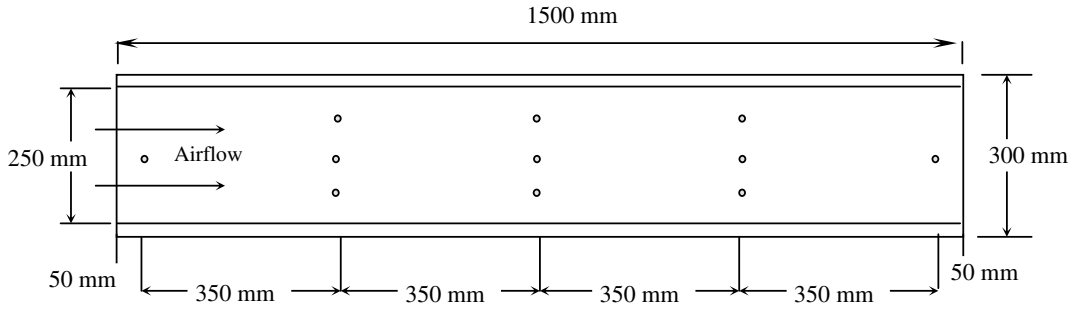

Fig. 2. The positions of the temperature sensors.

selected as 1.5 m. (Fig. 3) shows the layout of roughness surfaces of various geometries and (Table 1) gives the details of the roughness parameters.

A precision pyranometer was used for the measurement of the intensity of the solar radiation. The pyranometer is installed near the solar air heater with the horizontal guard plate of the pyranometer at the level of solar air heater. The measurement of wind velocity has been carried out using anemometer. The anemometer was installed in the vicinity of the collector at a height of the collector. All the data were recorded at an interval of half an hour from 10 am to 4 pm on clear days. This timing was selected to allow equal period of experimentation before and after solar noon.

4. Results and discussions

Fig. 4 shows the rate of useful energy gain and the power requirement of the fan as a function of Reynolds number. It is observed that the rate of increase of useful energy gain is relatively higher at low range of Reynolds number, whereas it is a bit lower at higher range of Reynolds number. But the rate of increase of power consumption is low for lower range of Reynolds number and increases relatively at high rate as Reynolds number increases. The power consumption does not exceed the rate of useful energy gain, i.e. the net energy gain rate is positive and it is also clear that at higher Reynolds number, the rate

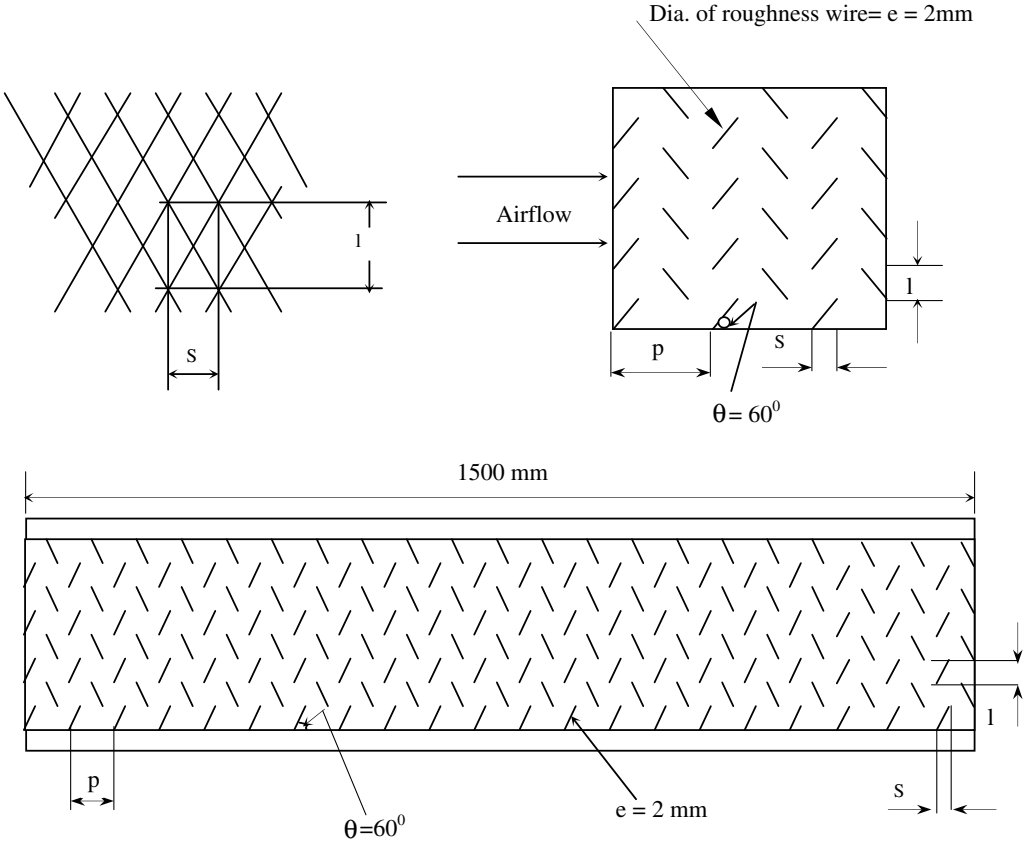

Plate No 02

Fig. 3. Layout of roughness surface.

Please cite this article in press as: Karmare, S.V., Tikekar, A.N., Experimental investigation of optimum thermohydraulic performance..., Sol. Energy (2008), doi:10.1016/j.solener.2008.05.017

Table 1
Details of the roughness parameters

Plate No	Pitch of metal grits, (mm) P	Diameter of metal grits, (mm) e	Rib angle of attack, degree (θ)	p/e	e/D_h	l/s
Plate No 01	Smooth plate					
Plate No 02	30	2.0	60	15.0	0.044	1.72
Plate No 03	28	1.6	60	17.5	0.035	1.72
Plate No 04	30	1.7	60	17.5	0.038	1.72

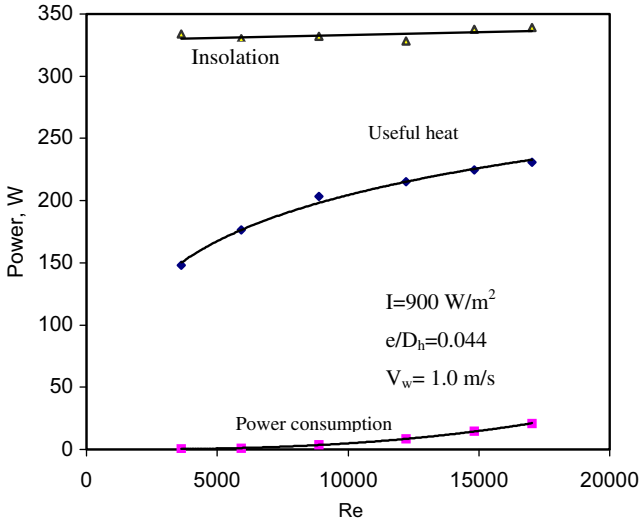

Fig. 4. Energy balance for solar collectors having roughened absorber plates.

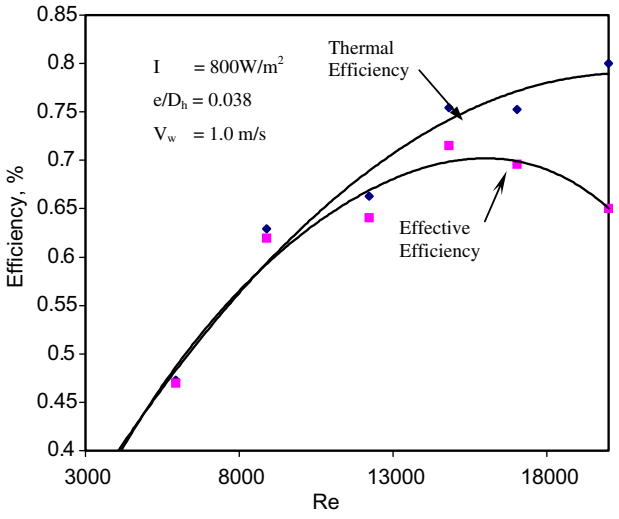

Fig. 5. Efficiency versus Reynolds number.

of useful energy collected becomes almost constant but the power consumption rises steeply.

The thermal as well as the effective efficiencies of the collector as a function of Reynolds number are shown in Fig. 5 which shows that the thermal efficiency increases with Reynolds number, whereas the effective efficiency attains a maximum value at a particular Reynolds number and thereafter decreases. This shows that an optimum operating condition does exist for the given roughness configuration at which the effective efficiency is maximum for a particular Reynolds number.

Fig. 6 shows the effective efficiency as a function of Reynolds number for different solar insolation. It is observed that for a particular value of insolation effective efficiency is maximum for a certain value of Reynolds number. As the value of insolation increases, the maximum value of effective efficiency shifts to higher Reynolds number. This leads to the conclusion that the flow should be adjusted to a Reynolds number so that the maximum effective efficiency for that value of insolation is ensured.

Fig. 7 shows useful energy collected (q_u) and power consumption (P_m/c) as a function of Reynolds number for different values of insolation. It reveals that the maximum value for the net energy gain shifts to a lower Reynolds number as the insolation decreases and hence the point of maximum effective efficiency also shifted to a lower Reynolds number. This appears due to a reduction in the plate

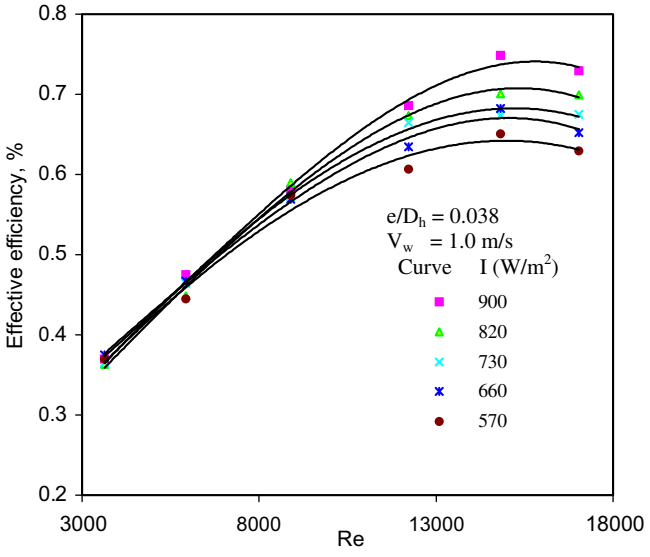

Fig. 6. Effective efficiency as a function of *Re* and Insolation.

temperature as the insolation decreases, lowers the rate of heat transfer to the air, whereas the power expenditure remains the same.

Fig. 8 shows the relation between insolation and effective efficiency for different Reynolds number. For Reynolds numbers 3630 and 5930, the effective efficiency decreases as insolation increases. However, for the values of Reynolds

Please cite this article in press as: Karmare, S.V., Tikekar, A.N., Experimental investigation of optimum thermohydraulic performance..., Sol. Energy (2008), doi:10.1016/j.solener.2008.05.017

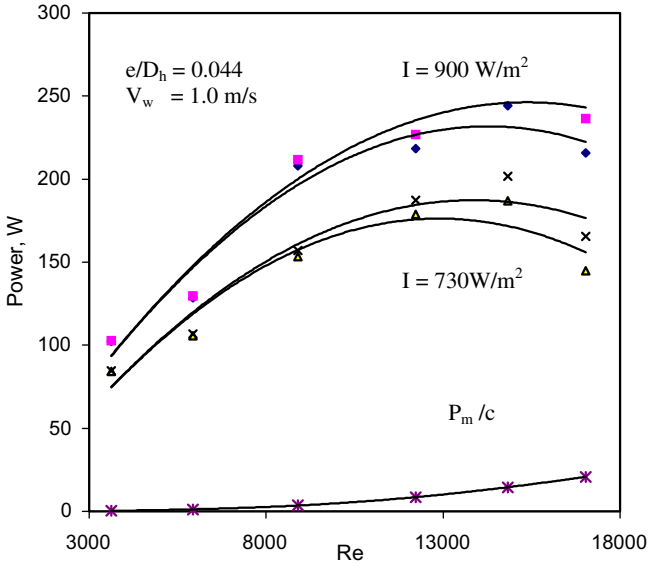

Fig. 7. Usefull energy and power consumption as a function of *Re* and different values of Insolation.

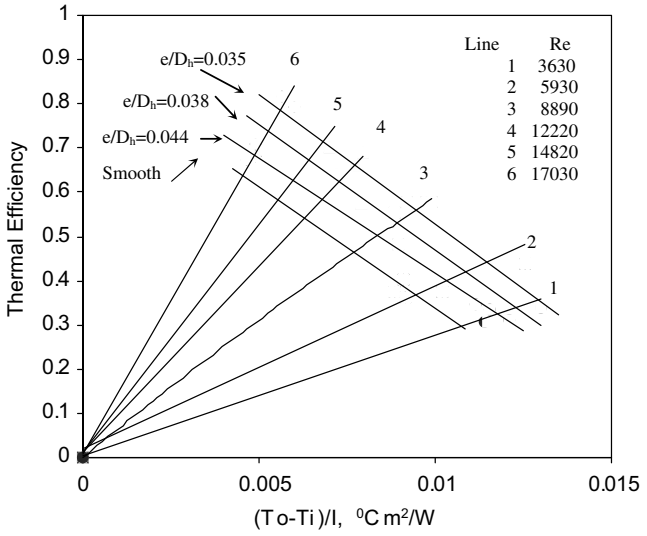

Fig. 9. Thermal efficiency versus thermal performance for different values of *Re* and e/D_h.

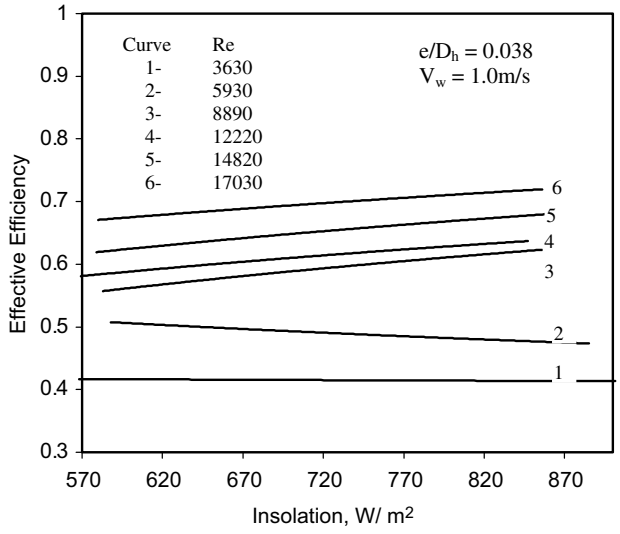

Fig. 8. Effective efficiency versus intensity of solar radiation for different values of *Re*.

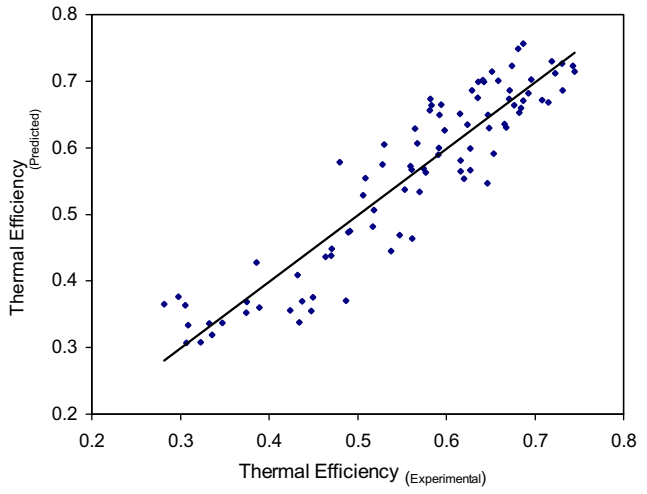

Fig. 10. Comparison of experimental values of thermal efficiency with predicted values.

numbers 8890 to 17030, the effective efficiency increases with increase in insolation

Fig. 9 shows the thermal efficiency versus $(T_o - T_i)/I$ for different values of Reynolds number and relative roughness height of roughened solar air heaters. It is observed that for a particular value of Reynolds number thermal efficiency increases with increase in $(T_o - T_i)/I$ at constant relative roughness height. It is also observed that thermal efficiency increases with relative roughness height.

The experimental values of thermal efficiency of the three roughened collectors are shown in Fig. 10. The predicted values of thermal efficiency are reasonably close to experimental values. The thermal efficiency lies within ± 8% with a standard deviation of ±6%.

5. Optimum design conditions

It has been demonstrated that the point of maximum effective efficiency depends strongly on roughness parameter and solar insolation. Reynolds number for optimum conditions also changes with roughness parameter and solar insolation. The performances of the solar air heater have been evaluated for a range of relative roughness height e/D_h:0.35–0.44, Reynolds number *Re*: 3600–17030 and solar insolation *I*: 570–900 W/m^2. (Fig. 11) shows the variation of the relative roughness height with Reynolds number for different values of solar insolation for optimum conditions and (Fig. 12) shows the relationship between the Reynolds number and solar insolation. (Table 2) shows the combinations of e/D_h, Reynolds number and solar insolation for optimum conditions of the operation of the solar

Please cite this article in press as: Karmare, S.V., Tikekar, A.N., Experimental investigation of optimum thermohydraulic performance..., Sol. Energy (2008), doi:10.1016/j.solener.2008.05.017

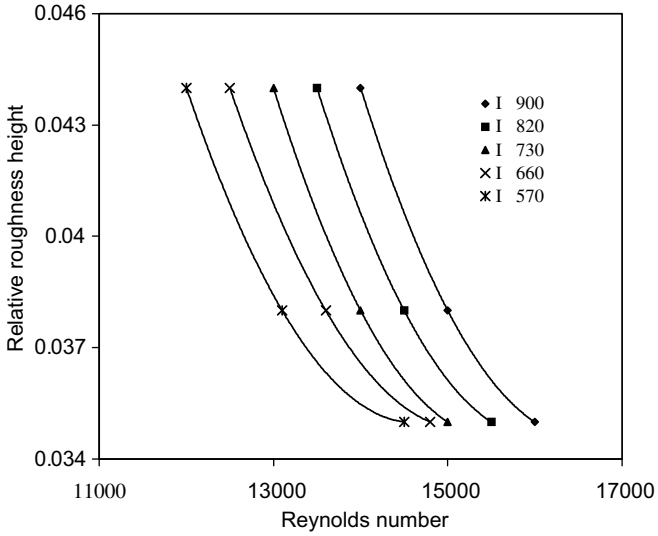

Fig. 11. Optimum conditions for a roughened solar air heater.

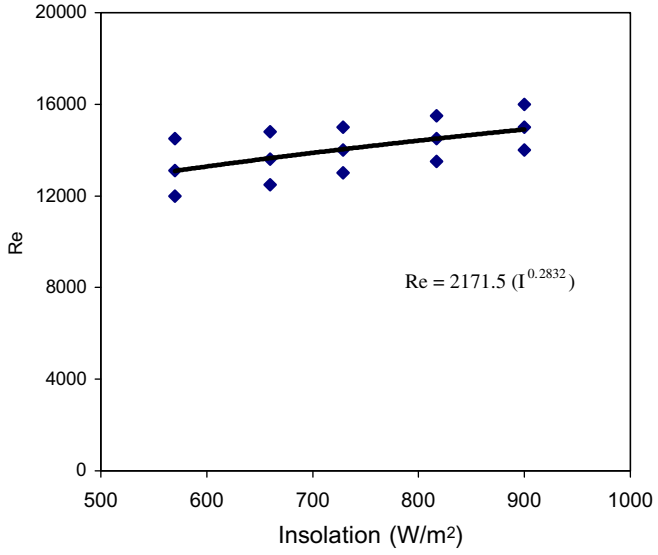

Fig. 12. *Re* versus intensity of solar radiation.

Table 2
Optimum conditions

e/D_h	Reynolds number				
	$I = 900$ W/m^2	$I = 820$ W/m^2	$I = 730$ W/m^2	$I = 660$ W/m^2	$I = 570$ W/m^2
0.035	16,000	15,500	15,000	14,800	14,500
0.038	15,000	14,500	14,000	14,300	13,100
0.044	14,000	13,500	13,000	13,500	12,000

air heater with metal rib grits roughness and the following empirical equation has been developed based on these data:

$$Re = 231(e/D_h)^{-0.69}(I)^{0.2832} \quad (12)$$

This equation correlates the data for optimum conditions with coefficient of determination ($R^2 = 0.92$) and standard deviation of 0.60%. It is recommended for use to determine the parameter values to achieve the maximum effective efficiency. The relationship between normalized roughness height and Reynolds number is shown in Fig. 13.

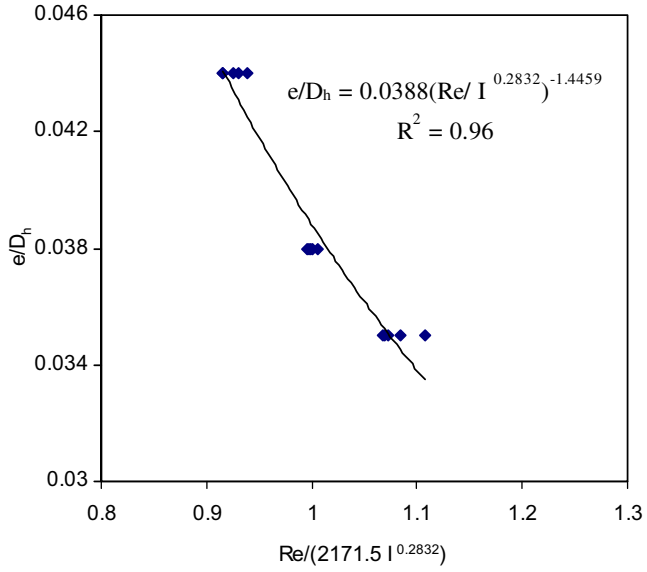

Fig. 13. Optimum condition curve for a roughed solar air heate

6. Conclusion

- The rate of increase of useful energy gain is relatively higher at low range of Reynolds number, whereas it is a bit lower at higher range of Reynolds number. But the rate of increase of power consumption is low for lower range of Reynolds number and increases relatively at high rate as Reynolds number increases.
- The optimum operating condition exists for the given roughness configuration at which the effective efficiency is maximum for a particular Reynolds number.
- The value of insolation increases, the maximum value of effective efficiency shifts to higher Reynolds number. This leads to the conclusion that the flow should be adjusted to a Reynolds number so that the maximum effective efficiency for that value of insolation is ensured.
- The thermal efficiency increases with relative roughness height.
- The predicted values of thermal efficiency are reasonably close to experimental values. The thermal efficiency lies within ±8% with a standard deviation of ±6%. Thus, the developed correlation can be utilized with confidence for the prediction of the performance of solar air heaters with metal rib grits on collector surface.
- The empirical relation which relates the system and operating parameters together to yield the optimum conditions is:

$$Re = 231(e/D_h)^{-0.69}(I)^{0.2832}$$

It is recommended for use to determine the parameter values to achieve the maximum effective efficiency.

Please cite this article in press as: Karmare, S.V., Tikekar, A.N., Experimental investigation of optimum thermohydraulic performance..., Sol. Energy (2008), doi:10.1016/j.solener.2008.05.017

7. Uncited references

Cortes and Piacentini (1990) and Kline and McClintiok (1953).

Acknowledgements

Government College of Engineering, Karad and Rajarambapu Institute of Technology, Rajaramnagar, Sakharale supported this research. The authors acknowledge both these institutes for providing facilities.

References

ASHRAE standard 93-77, 1977. Method of testing of determines thermal performance of solar collector.

Cortes, A., Piacentini, R., 1990. Improvement of the effective efficiency of a bare solar collector by means of turbulence promoters. Appl. Energy. 36, 253–256.

Dhananjay, Gupta, Solanki, S.C., Saini, J.S., 1997. Thermo hydraulic performance of solar air hearers with roughened absorber plates. Solar Energy 61, 33–42.

Dipprey, D.F., Sabersky, R.H., 1963. Heat and momentum in smooth and rough tubes at various Prandtl numbers. Int. J. Heat Mass Transfer 6, 329–353.

Han, J.C., 1984. Heat transfer and friction in a channel with two opposite rib roughened walls. Int. J. Heat Transfer 106, 774–781.

Han, J.C., Zhang, Y.M., 1992. High performance heat transfer ducts with parallel broken V shaped broken ribs. Int. J. Heat Mass Transfer 35, 513–523.

Hosni, M.H., Hugh, W.C., Robert, P.T., 1991. Measurement and calculations of rough wall heat transfer in the turbulent boundary layer. Int. J. Heat Mass Transfer 34, 1067–1082.

Karmare, S.V., Tikakar, A.N., 2007. Heat transfer and friction factor correlation for artificially Roughened duct with metal grit ribs. Int. J. Heat Mass Transfer 50, 4342–4351.

Karwa, R., Solanki, S.C., Saini, J.S., 1999. Heat transfer coefficient and friction factor correlation for the transitional flow regime in rib roughened rectangular ducts. Int. J. Heat Mass Transfer 42, 1597–1615.

Kline, S.J., McClintiok, F.A., 1953. Describing uncertainties in single sample experiments. Mech. Eng. 75, 3–8.

Liou, T., Hwang, J., 1993. Effect of ridge shapes on turbulent heat transfer and friction in a rectangular channel. Int. J. Heat Mass Transfer 36, 93–140.

Prasad, K., Mullick, S., 1983. Heat transfer characteristics of a solar air heater used for drying purposes. Appl. Energy 13, 83–98.

Prasad, B.N., Saini, J.S., 1988. Effect of artificial roughness on heat transfer and friction factor in solar air heater. Solar Energy 41, 555–560.

Saini, R.P., Saini, J.S., 1997. Heat transfer and friction factor correlations for artificially roughened duct with expanded metal mesh as roughness element. Int. J. Heat Mass Transfer 40, 973–986.

Webb, R.L., Eckert, E.R.G., 1972. Application of rough surfaces of heat exchanger design. Int. J. Heat Mass Transfer 5, 1647–1658.